Low-temperature Scanning Tunneling Microscopy and Spectroscopy of Noble-metal Surfaces*

Erik Zupanič,[a,**] Rok Žitko,[a] Herman J. P. van Midden,[a] Igor Mušević,[a,b] and Albert Prodan[a]

[a]*Jožef Stefan Institute, Jamova 39, SI-1000 Ljubljana, Slovenia*
[b]*Faculty of Mathematics and Physics, University of Ljubljana, SI-1000 Ljubljana, Slovenia*

Abstract. Low-index surfaces of copper single crystals were studied by scanning tunneling microscopy (STM) and spectroscopy (STS). The experiments were performed under ultra-high vacuum conditions at room- and close to liquid helium- temperatures. At lower temperatures thermal drifts are largely reduced, a better STM mechanical stability is achieved and improved spectroscopy measurements, with the energy resolution shifted from meV to µeV, are possible. Low-index surfaces of bulk copper single crystals are unstable at room temperature and show poor atomic resolution with unstable single-atomic steps. In order to reduce thermal vibrations and improve atomic resolution, such surfaces must be cooled close to liquid helium temperature. At cryogenic temperatures individual surface defects, adsorbents and electronic standing waves can be studied. In addition, individual adatoms can be manipulated by STM into desired nanostructures and analyzed by STS. By measuring $dI/dU(U)$, which is proportional to the local density of states, spectroscopic information with high spatial resolution can be obtained.

Keywords: STM, STS, noble metals, manipulation

INTRODUCTION

Single crystal surfaces of noble metals are intensively studied nowadays because of their importance as substrates in surface manipulation and restructuring experiments.[1–4] Noble-metal deposits on other noble-metals[5,6] as well as deposits of magnetic metals on noble-metals[7–11] were intensively studied by scanning tunneling microscopy (STM) and related methods. Atomic and molecular adsorption on these substrates is likewise of great importance for catalysis. Such studies included adsorption of elements like H, O, N, S and C on Pt(111)[12] and N on Cu(001),[13] but also deposits of simple molecules like NO_2 on Ag(111),[14] SO_2 on Cu(110)[15] and CO on Ag(111),[16] Ag(221)[17] and Cu(111).[18] Further, STM was intensively employed to study the behavior of more complicated molecules on noble-metal surfaces[19–30] and to investigate hetero-epitaxial growth of inorganic compounds, like MoO_3 on Au(111).[31] Reverse combinations, *i.e.* deposits of noble-metals on layered inorganic compounds, mostly transition-metal dichalcogenides,[32–34] with particular emphasis on postintercalation of the deposits into the van der Waals (vdW) gaps of the substrates[35,36] were also investigated.

STM and scanning tunneling spectroscopy (STS) were applied to study the metallic surfaces on an atomic level. While STM reveals the topography of the surface, STS allows measurement of the local density of states (LDOS) and the energy gaps, either of the surface itself or the adsorbates on it. Because of the sharp tip used, the tunneling current is limited to areas of the order of 0.5 nm^2, which makes STS sensitive to several orders of magnitude smaller regions in comparison with any other spectroscopic method. Although atomic resolution can be routinely achieved with STM at room temperature (RT), cooling the sample and the STM to cryogenic temperatures results in more stable tunneling and reduced thermal drifts. It also enables studies of specific low temperature phenomena and guaranties, due to reduced thermal broadening of the linewidths, an improved energy resolution in STS measurements.[37–39]

In the present study the properties of bulk copper single crystal (111) and (211) surfaces are described. We are particularly interested in structural aspects of the

---

surfaces, like *e.g.* its stability at room-temperature, but also in the role of various surface defects, like point defects with the accompanied electronic standing waves, which characterize these surfaces at reduced temperatures. Further, extraction of individual Cu atoms and their manipulation into different arrangements is described and the ability of STS as a spectroscopic method is demonstrated in case of individual Cu ad-atoms on the Cu(111) surface.

EXPERIMENTAL

High purity copper single crystal surfaces with (111) and (211) orientations were purchased from Surface preparation laboratory, The Netherlands. Electro-polished samples were cleaned during repeated (3–10) in-situ heating ($T = 920$ K) and ion-beam etching (1 keV Ar^+ ions, $J_{ion} = 10$ μA/cm^2) cycles. The crystallography and chemistry of the surfaces were controlled by low-energy electron diffraction (LEED) and Auger spectro-scopy (AES), respectively. STM constant-current (CCM) and constant-height mode (CHM) measurements were performed at RT and close to liquid helium (LHe) temperature under ultra-high vacuum conditions (10^{-8}–10^{-9} Pa). $dI/dU(U)$ spectra were measured at chosen surface positions with a digital lock-in amplifier (Stan-ford Research R830) . The STS measurement was per-formed by bringing the tip into the required position, where the feed-back loop was opened and the $dI/dU(U)$ spectra measured at a constant tip-surface distance. Sharp and stable tungsten tips for STM and STS were prepared by electronically controlled electro-chemical etching in 2 mol dm^{-3} KOH. Bias voltages refer to the sample voltage with respect to the tip. Due to a low corrugation in some STM images, removal of the low-frequency noise by means of a low-pass filter, flattening and contrast enhancement were necessary to show up features of interest. STS curves are shown as recorded.

RESULTS

In case of low-index single crystal copper surfaces, STM images recorded at RT show atomic resolution on clean and completely flat surfaces only. If present, atomic steps are unstable and change their shapes during subsequent scans. By cooling the specimen close to the LHe temperature the surface is thermodynamically stabi-lized and the resolution is accordingly improved. Con-trary to the Cu(111) surfaces (Figures 1 and 2) the cor-rugated Cu(211) surfaces show elongated atomic steps, with periodic ridges and groves along the [0-11] direc-tion of the exposed surface layer (Figure 3). Individual copper atoms are often displaced from their equilibrium
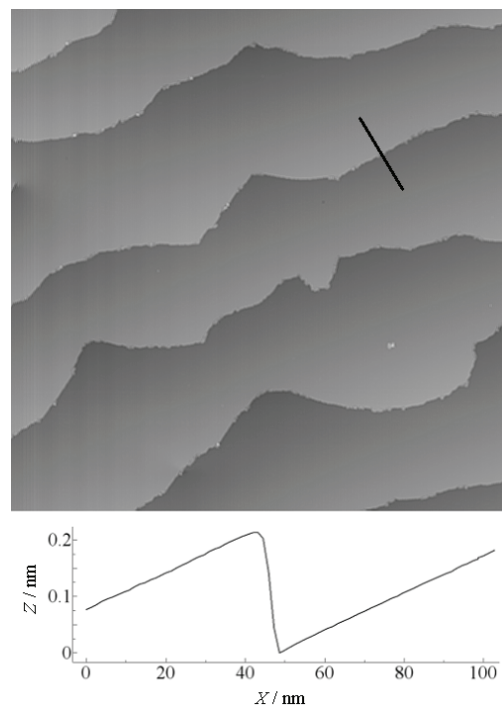

Figure 1. Low-magnification STM image of a Cu(111) sur-face, recorded at 9 K. The line profile reveals single-atom surface step, 0.21 nm high (CCM, 500 nm^2, $I_t = 0.47$ nA, $U_t = 100$ mV, $T = 10$ K).
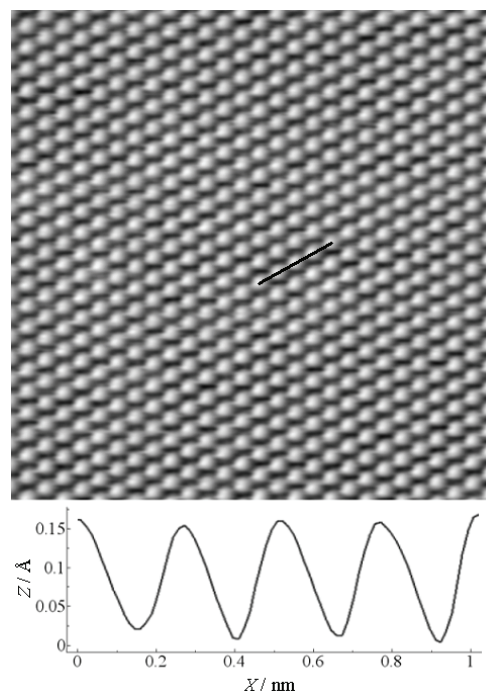

Figure 2. High-resolution STM image of an ideal Cu(111) surface with a line-profile revealing the 0.25 nm periodicity between individual Cu atoms (CCM, 6.3 nm^2, $I_t = 2.6$ nA, $U_t = 170$ mV, $T = 9$ K).
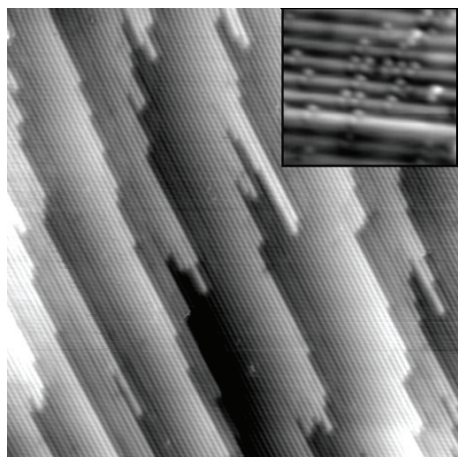
Figure 3. STM image of a Cu (211) corrugated surface, characterized by (111) nanofacets with ridges and groves along the [0-11] direction (38 nm^2, CCM, $I_t = 0.7$ nA, $U_t = 805$ mV, $T = 7$ K). Single Cu atoms, displaced from their equilibrium positions in the topmost atom chains can be seen in the inset.

positions in the uppermost copper chains, as shown in the inset of Figure 3. These are probably a result of ion etching and insufficient annealing during the cleaning procedure. In addition to atomic resolution, the atomically flat Cu(111) surfaces often show at reduced temperatures structures, formed of different adsorbates, CO molecules adsorbed from residual gases (Figures 4a and 4b), agglomerates of adatoms at atomic steps, groups of atomic vacancies, and electronic standing waves at surface and subsurface point defects. The W tips used were for two reasons on purpose intruded in a controlled manner into the clean Cu surfaces. In this way the apex of the tip was preconditioned until it was terminated by a single Cu atom. Second, single Cu ad-atoms were produced in this way on the substrate surface (Figure 5).
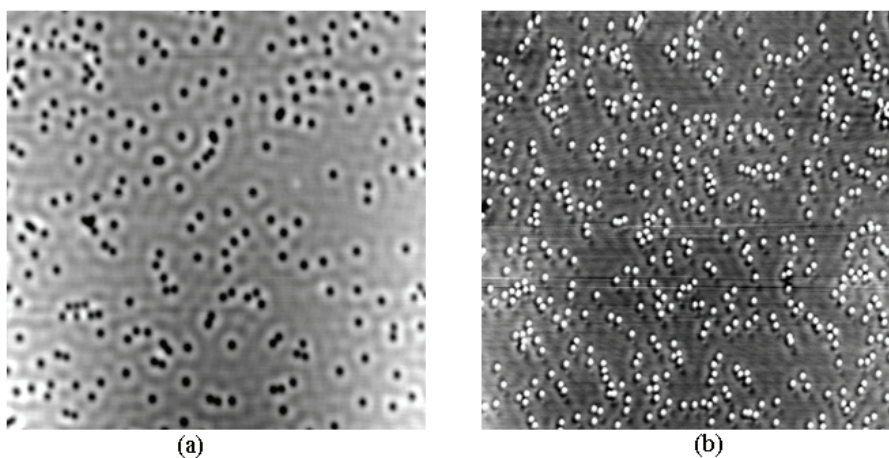
Single atoms can be distinguished from their agglomerates, as shown in the inset of Figure 5. While individual atoms are always the smallest round shaped species, doublets are unstable and appear slightly blurred due to their permanent rotation,[40] while triplets are considerably larger. Individual Cu atoms produced in this way can be manipulated at low tempe-ratures by the same STM tip by precisely controlling the quantum mechanical interactions. The constant height mode lateral manipulation procedure involves exact positioning of the tip over the adatom, reduction of the distance between the tip and the adatom (resulting in stronger attractive forces), displacement of the tip (and the adatom) along a chosen path in a constant height mode, and finally retraction of the tip to the initial imaging height.[41,42] An example is shown in Figures 6a and 6b, where the "IJS" initials and a "smiley" are shown. Electronic standing waves of small amplitudes are clearly visible in Figure 6b. At a low bias voltage U_t the constant current image can be interpreted as an image of the LDOS at an energy eU_t above the Fermi level (E_F). For a simple free electron like surface state, standing waves with a wave vector $2k_F$ can be observed (Figure 7a). Since the STM is sensitive to the square of the wavefunction ψ the wavelength of the wave vector appears half shorter. The wave vector k_F is extracted from the 2D Fourier-transform of the corresponding STM image (Figure 7b). A wavelenght λ_F of 1.4 nm was measured for the surface state electrons at E_F, which is in accord with previously published data.[43]

STS measurements were performed on clean Cu (111) surfaces as well as on individual Cu adatoms. In Figure 8 a high-resolution STM image of an individual Cu atom on a Cu(111) surface is shown with two series of STS spectra recorded at the indicated positions. The spectra recorded on a clean and flat surface are in ac-

(a)   (b)

Figure 4. CO molecules on a Cu(111) surface. The molecules appear black in case of a clean Cu tip (a) (CCM, 62.5 nm^2, $I_t = 1.0$ nA, $U_t = 211$ mV, $T = 25$ K) or white, if the tip is terminated by a CO molecule (b) (CCM, 75 nm^2, $I_t = 1.1$ nA, $U_t = 211$ mV, $T = 25$ K).
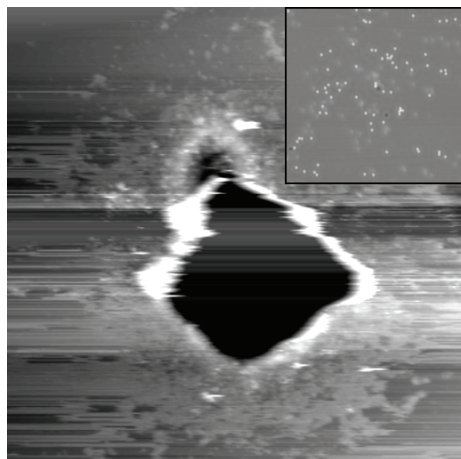
Figure 5. Low-temperature STM image of a Cu(111) surface acquired after a W tip was dipped into it. Scattered individual Cu adatoms around the crash site can be seen in the inset. (CCM, 160 nm^2, $I_t = 0.30$ nA, $U_t = 96$ mV , $T = 9$ K, inset 30 nm^2).

cord with some recent measurements and show a clear depletion in the LDOS spectra at about 450 mV below the Fermi energy (E_F), which was interpreted as the band edge of the copper surface state.[44] In case the measurements are performed in a wider range, *i.e.* between –3 V and +3 V, more such depletions are clearly detected at different energies. It was shown previously that the width Δ of the onset in Figure 7 is directly related to the lifetime of the holes at the surface state band-edge.[45] The measured width Δ of 37 mV and the calculated lifetime τ of 22 fs are in good agreement with previous measurements.[46] The spectra recorded on isolated copper adatom exhibit a clear peak at 490 mV below E_F with a full-width at half-maximum (FWHM) of 150

mV, which shows the presence of an adatom induced localization of the surface state.[37]

In addition to spectra measured on the Cu(111) surface and on the individual Cu adatom STS was also performed along the 15 points marked in the inset of Figure 9. The characteristic resonance peak in the spectra vanishes rapidly in a continuous manner with the increasing distance from the Cu adatom. At about 2.5 nm from the adatom only the characteristic edge of the Cu(111) surface states is detected.

DISCUSSION

Contrary to all other up-to-date microscopic methods, including high-resolution transmission electron microscopy, various scanning probe microscopies represents the only methods able to reveal single atoms and molecules in real space and real time. Stability and mobility of the surface Cu atoms are strongly influenced by the tip-sample interaction. While the tunneling currents used in STM and STS experiments are as low as nA and below, they are spatially limited to areas of the order of single atoms, which results in huge current densities. The imaging resolution is also limited by thermal vibrations and mechanical drifts, caused by temperature gradients. To improve the spatial and energy resolution the experiments are to be performed at temperatures as low as possible. Close to the LHe temperature STM clearly reveals in addition to the periodic surface structure a variety of adsorbates, impurities, point defects and related phenomena, like electronic standing waves. If the experiments are performed in an extremely clean environment and at sufficient low temperatures, the mentioned structural imperfections are routinely detected.
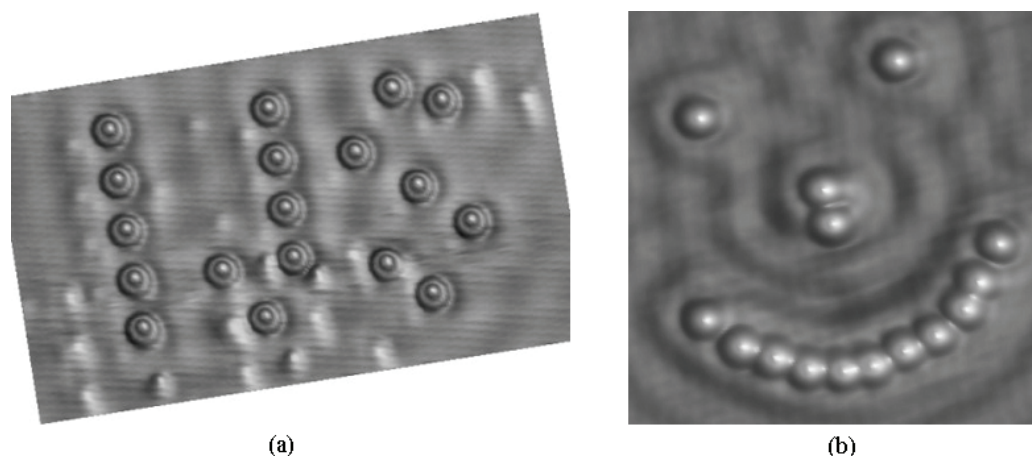

(a)   (b)

Figure 6. Initials "IJS" (a) (CCM, 15×9 nm, $I_t = 0.8$ nA, $U_t = 96$ mV , $T = 9$ K) and "smiley" (b) (CCM, 11 nm^2, $I_t = 0.8$ nA, $U_t = 96$ mV , $T = 9$ K) formed of manipulated individual Cu adatoms on a Cu(111) surface.

(a)   (b)
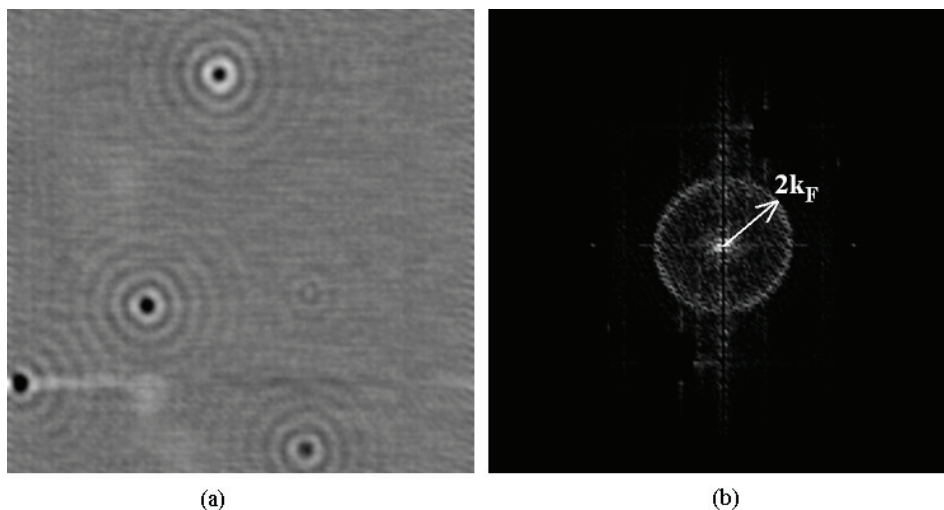
Figure 7. (a) Constant current image of a Cu(111) surface with point defects and low amplitude standing electron waves with a wave vector $2k_F$ (CCM, 37×37 nm, $I_t = 1.5$ nA, $U_t = 50$ mV , $T = 9$ K). (b) The power spectrum of the 2D Fourier transform of (a) provides a direct image of the Fermi contour.

The different modes of STM operation and the variability of the parameters used, make a few local spectroscopies possible. The STS spectra, based on the dependence of the tunneling current on the gap voltage at a constant tip-surface separation, show an excellent reproducibility, which can be followed into the finest details of the spectra recorded. However, there is also a disadvantage, which makes these measurements tedious. These spectra depend on both, the shape and the chemistry of the particular tip used and the wave functions involved. Unfortunately, the actual shape of the tip is not known on an atomic scale. Thus, certain precautions

are to be undertaken before unknown spectra are measured. In the present case, the tip was repeatedly intruded into the Cu surface in a controlled way, until the STS spectra measured on the Cu(111) surface verifies characteristic features such as the surface state band edge and no sharp peaks around zero bias.[37] That was the only assurance that the apex of the tip was covered by Cu atoms and approximately round-shaped. Only with such a tip measurements on single Cu adatoms were undertaken. The measured spectra show a characteristic small peak at about 50 mV below the deep edge at –450 mV, attributed to the Cu(111) surface states. This peak vanishes rapidly with distance and is completely lost at about 2.5 nm from the centre of the ad-
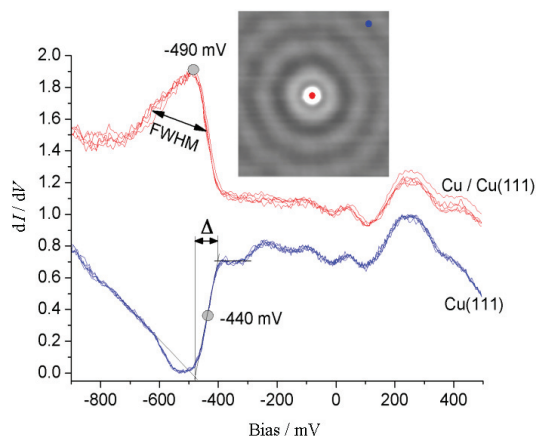

Figure 8. Two series of differential conductance spectra dI/dV, measured on a clean Cu(111) surface (blue) and on an isolated Cu adatom on Cu(111) surface (red). The circles in the inset mark the respective tip positions during the measurements. The width Δ of the onset is directly related to the lifetime of the electronic states.
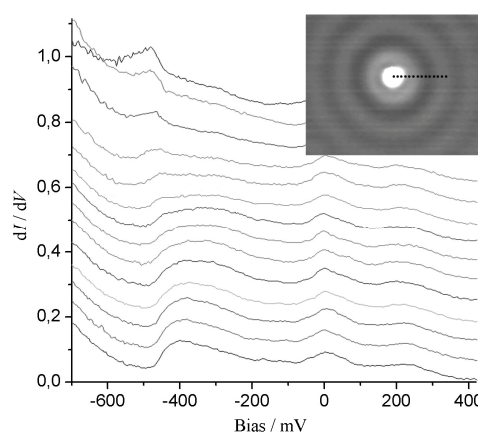

Figure 9. Differential conductance spectra dI/dV, measured on the 15 marked points, displaced by 0.2 nm. With increasing lateral tip displacement from the adatom the localization peak at –490 mV rapidly decays in intensity and the copper surface state band edge at a sample bias at –440 mV evolves.

atom. The surface-state lifetime in combination with the velocity determines the mean free path of the surface-state electrons and hence the effective excitation range. An advantage of measuring lifetimes with STM is the ability to verify surface quality before taking spectroscopy measurements and thus avoid effects from different defects. The lifetime τ for the states at the surface-state band edge on Cu(111) was measured to be 22 fs.

The described experiments represent a clear proof that STM and STS are two related methods, sufficiently accurate and sensitive to allow microscopic and spectroscopic measurements on an atomic scale and below. It is expected that characteristic spectra, measured on a variety of surface species, will gain importance in future nanotechnological processes and will enable identification of individual species, important for the local surface properties.

CONCLUSIONS

The quality of the STM images and the STS spectra depend largely on the shape of the tip. While STM requires as sharp as possible tips, best STS measurements are performed with slightly blunt tips, which show less sharp peaks in tip DOS and ensure a better reproducibility of the spectra measured.

Cu(111) and (211) single crystal surfaces are unstable during scanning at room temperature. Reduced temperatures reduce thermal vibrations and largely improve the STM resolution.

Single crystal Cu(111) surfaces, recorded at LHe temperature and under UHV conditions, are characterized by impurities, adsorbed CO molecules, and electronic standing waves localized at surface and subsurface point defects. The wavelenght λ_F of the surface state electrons at E_F was measured to be 1.4 nm.

Cu(211) single crystal surfaces reveal irregular atomic steps, elongated along the periodic surface ridges and groves and often reveal single Cu atoms, displaced from their equilibrium positions in the uppermost Cu chains.

STS performed on a clean and flat Cu(111) surface reveals a large depletion in LDOS at 450 mV below E_F, which is attributed in accord with literature to the edge of the electronic surface state band structure. The lifetime τ for the holes at the surface state band-edge was measured to be 22 fs.

STS of single Cu adatoms reveals a characteristic peak in LDOS some 50 mV below the edge of the surface electronic states with a FWHM of 150 mV, attributed to localization of the Cu(111) surface state. The peak vanishes rapidly with the distance from the ad-atom.

REFERENCES

1. S. Fölsch, P. Hyldgaard, R. Koch, and K. H. Ploog, *Phys. Rev. Lett.* **92** (2004) 056803-1-4.
2. N. Quaas, M. Wenderoth, and R. G. Ulbrich, *Surf. Sci.* **550** (2004) 57–64.
3. X. Zhao, S. S. Perry, and J. D. Horvath, and A. J. Gellman, *Surf. Sci.* **563** (2004) 217–224.
4. G. Grochola, J. Du Plessis, I. K. Snook, and S. P. Russo, *Surf. Sci.* **591** (2005) 32–7.
5. C. Maurel, M. Abel, M. Koudia, F. Bocquet, and L. Porte, *Surf. Sci.* **596** (2005) 45–52.
6. H. Cercellier, C. Didiot, Y. Fagot-Revurat, B. Kierren, L. Moreau, and D. Malterre, *Phys. Rev. B* **73** (2006) 195413-1-16.
7. C. Goyhenex, *Surf. Sci.* **600** (2006) 15–22.
8. P. Allongue, L. Cagnon, C. Gomes, A. Gündel, and V. Costa, *Surf. Sci.* **557** (2004) 41–56.
9. M. M. Biener, J. Biener, R. Schalek, and C. M. Friend, *Surf. Sci.* **594** (2005) 221–227.
10. A. Bergman, L. Nordström, A. Burlamaqui Klautau, S. Frota-Pessôa, and O. Eriksson, *Phys. Rev. B* **73** (2006) 174434-1-5.
11. O. Pietzsch, S. Okatov, A. Kubetzka, M. Bode, S. Heinze, A. Lichtenstein, and R. Wiesendanger, *Phys. Rev. Lett.* **96** (2006) 237203-1-4.
12. D. C. Ford, Y. Xu, and M. Mavrikakis, *Surf. Sci.* **587** (2005) 159–174.
13. S. Ohno, K. Yagyuu, K. Nakatsuji, and F. Komori, *Surf. Sci.* **547** (2003) L871–L876.
14. A. R. Alemozafar and R. J. Madix, *Surf. Sci.* **587** (2005) 193–204.
15. A. R. Alemozafar, X.-C. Guo, and R. J. Madix, *Surf. Sci.* **524** (2003) L84–L88.
16. M. Kulawik, H.-P. Rust, M. Heyde, N. Nilius, B. A. Mantooth, P. S. Weiss, and H.-J. Freund, *Surf. Sci.* **590** (2005) L253–L258.
17. J. Lee, J.-G. Lee, and J. T. Yates Jr., *Surf. Sci.* **594** (2005) 20–26.
18. M. Neef and K. Doll, *Surf. Sci.* **600** (2006) 1085–1092.
19. R. Nowakowski, C. Seidel, and H. Fuchs, *Surf. Sci.* **562** (2004) 53–64.
20. G.-J. Su, S.-X. Yin, L.-J. Wan, J.-C. Zhao, and C.-L. Bai, *Surf. Sci.* **551** (2004) 204–212.
21. J. Nieminen, E. Niemi, V. Simic-Milosevic, and K. Morgenstern, *Phys. Rev. B* **72** (2005) 195421-1-8.
22. C. Matsumoto, Y. Kim, T. Okawa, Y. Sainoo, and M. Kawai, *Surf. Sci.* **587** (2005) 19–24.
23. L. Grill, K.-H. Rieder, F. Moresco, G. Jimenez-Bueno, C. Wang, G. Rapenne, and C. Joachim, *Surf. Sci.* **584** (2005) L153–L158.
24. K. Tsukamoto, T. Kubo, and H. Nozoye, *Appl. Surf. Sci.* **244** (2005) 578–583.
25. A. Kirakosian, M. J. Comstock, J. Cho, and M. F. Crommie, *Phys. Rev. B* **7** (2005) 113409-1-4.
26. L. Gross, F. Moresco, P. Ruffieux, A. Gourdon, C. Joachim, and K.-H. Rieder, *Phys. Rev. B* **71** (2005) 165428-1-7.
27. M. J. Comstock, J. Cho, A. Kirakosian, and M. F. Crommie, *Phys. Rev. B* **72** (2005) 153414-1-4.
28. L. Gross, K.-H. Rieder, F. Moresco, S. M. Stojkovic, A. Gourdon, and C. Joachim, *Nat. Mate.* **4** (2005) 892–895.

29. D. X. Shi, W. Ji, X. Lin, X. B. He, J. C. Lian, L. Gao, J. M. Cai, H. Lin, S. X. Du, F. Lin, C. Seidel, L. F. Chi, W. A. Hofer, H. Fuchs, and H.-J. Gao, *Phys. Rev. Lett.* **96** (2006) 226101-1-4.

30. W. Auwärter, A. Weber-Bargioni, A. Rieman, A. Schiffrin, O. Gröning, R. Fasel, and J. V. Barth, *J. Chem. Phys.* **124** (2006) 194708-1-6.

31. M. M. Biener and C. M. Friend, *Surf. Sci.* **559** (2004) L173–L179.

32. S. W. Hla, V. Marinković, and A. Prodan, *Surf. Sci.* **356** (1996) 130–136.

33. S. W. Hla, V. Marinković, and A. Prodan, *Surf. Sci.* **377–379** (1997) 979–982.

34. C. Maurel, F. Ajustron, R. Péchou, G. Seine, and R. Coratger, *Surf. Sci.* **600** (2006) 442–447.

35. A. Prodan, V. Marinković, M. Rojšek, N. Jug, H. J. P. van Midden, F. W. Boswell, J. C. Bennett, and H. Böhm, *Surf. Sci.* **476** (2001) 71–77.

36. E. Spiecker, A. K. Schmid, A. M. Minor, U. Dahmen, S. Hol-lensteiner, and W. Jäger, *Phys. Rev. Lett.* **96** (2006) 086401-1-4.

37. F. E. Olsson, M. Persson, A. G. Borisov, J.-P. Gauyacq, J. Lagoute, and S. Fölsch, *Phys. Rev. Lett.* **93** (2004) 206803-1-4.

38. J. Tersoff and D. R. Hamann, *Phys. Rev. B* **31** (1985) 805–813.

39. N. D. Lang, *Phys. Rev. B* **34** (1986) 5947–5950.

40. J. Repp, G. Meyer, K.-H. Rieder, and P. Hyldgaard, *Phys. Rev. Lett.* **91** (2003) 206102-206-1-4.

41. S. W. Hla, K.-F. Braun, and K.-H. Rieder, *Phys. Rev. B* **67** (2003) 201402(R)-1–4.

42. S. W. Hla, *J. Vac. Sci. Technol.*, *B* **23** (2005) 1351–1360.

43. M. F. Crommie, C. P. Lutz, and D. M. Eigler, *Nature* **363** (1993) 524–527.

44. A. G. Borisov, A. K. Kazansky, and J. P. Gauyacq, *Phys. Rev. B* **65** (2002) 205414-1–7.

45. J. Li, W.-D. Schneider, R. Berndt, O. R. Bryant, and S. Crampin, *Phys. Rev. Lett.* **81** (1998) 4464.

46. J. Kliewer, R. Berndt, E. V. Chulkov, V. M. Silkin, P. M. Echenique, and S. Crampin, *Science* **288** (2000) 1399.

SAŽETAK

Niskotemperaturna pretražna tunelirajuća mikroskopija i spektroskopija ploha plemenitih kovina

Erik Zupanič,[a] Rok Žitko,[a] Herman J. P. van Midden,[a] Igor Mikušević[a,b] i Albert Prodan[a]

[a]*Jožef Stefan Institute, Jamova 39, SI-1000 Ljubljana, Slovenia*
[b]*Faculty of Mathematics and Physics, University of Ljubljana, SI-1000 Ljubljana, Slovenia*

Niskotemperaturnom pretražnom tunelirajućom mikroskopijom (STM) i spektroskopijom (STS) istraživane su plohe monokristala bakra malih indeksa. Mjerenja su izvedena u uvjetima vrlo visokog vakuuma pri sobnoj temperaturi i blizu temperature tekućeg helija. Na niskim su temperaturama znatno smanjene termičke smetnje, te je ostvarena bolja mehanička stabilnost STM slike, odnosno poboljšana su spektroskopska mjerenja uz povećanje energijskog razlučivanja od meV prema μeV. Plohe masivnih monokristala bakra malih indeksa su nestabilne na sobnoj temperaturi i pokazuju slabo razlučivanje na atomskoj ljestvici. U svrhu smanjenja termičkog titranja i poboljšanja razlučivanja na atomskoj ljestvici, takve se plohe moraju hladiti na temperature blizu onima tekućeg helija. Na tim je temperaturama moguće proučavati pojedine površinske defekte, adsorbense i stojne valove elektrona. Uz to je, pomoću STM moguće micati dodatne pojedinačne atome, stvarati željene nanostrukture i analizirati ih pomoću STS. Mjerenjem vrijednosti dI/dU(U), koja je razmjerna lokalnoj gustoći stanja, mogu se dobiti spektroskopijske informacije visokog prostornog razlučivanja.